Published in final edited form as:
J Immunol. 2011 April 1; 186(7): 4422–4432. doi:10.4049/jimmunol.1002324.

Rapid Recruitment and Activation of Macrophages by Anti-Gal/α-Gal Liposome Interaction Accelerates Wound Healing

Kim M. Wigglesworth[*], **Waldemar J. Racki**[†], **Rabinarayan Mishra**[‡], **Eva Szomolanyi-Tsuda**[‡], **Dale L. Greiner**[†], and **Uri Galili**[*]

[*]Department of Surgery, University of Massachusetts Medical School, Worcester, MA 01655

[†]Department of Medicine, University of Massachusetts Medical School, Worcester, MA 01655

[‡]Department of Pathology, University of Massachusetts Medical School, Worcester, MA 01655

Abstract

Macrophages are pivotal in promoting wound healing. We hypothesized that topical application of liposomes with glycolipids that carry Gala1-3Galb1-4GlcNAc-R epitopes (α-gal liposomes) on wounds may accelerate the healing process by rapid recruitment and activation of macrophages in wounds. Immune complexes of the natural anti-Gal Ab (constituting ~1% of Ig in humans) bound to its ligand, the α-gal epitope on α-gal liposomes would induce local activation of complement and generation of complement chemotactic factors that rapidly recruit macrophages. Subsequent binding of the Fc portion of anti-Gal coating α-gal liposomes to FcγRs on recruited macrophages may activate macrophage genes encoding cytokines that mediate wound healing. We documented the efficacy of this treatment in α1,3galactosyltrasferase knockout mice. In contrast to wild-type mice, these knockout mice lack α-gal epitopes and can produce the anti-Gal Ab. The healing time of excisional skin wounds treated with α-gal liposomes in these mice is twice as fast as that of control wounds. Moreover, scar formation in α-gal liposome-treated wounds is much lower than in physiologic healing. Additional sonication of α-gal liposomes resulted in their conversion into submicroscopic α-gal nanoparticles. These α-gal nanoparticles diffused more efficiently in wounds and further increased the efficacy of the treatment, resulting in 95–100% regeneration of the epidermis in wounds within 6 d. The study suggests that α-gal liposome and α-gal nanoparticle treatment may enhance wound healing in the clinic because of the presence of high complement activity and high anti-Gal Ab titers in humans.

Macrophages are pivotal cells in orchestrating the healing of wounds and internal injuries (1–6). Macrophages debride wounds and phagocytose and destroy invading bacteria. Macrophages are further activated within the wound to secrete a variety of cytokines that recruit additional cells and induce their proliferation, thereby promoting regeneration of the injured tissue. Injection of activated macrophages into wounds of patients was reported to promote wound healing (7). These data led to the hypothesis that induction of rapid in situ

Address correspondence and reprint requests to Dr. Uri Galili, Department of Surgery, HB774, University of Massachusetts Medical School, 55 Lake Avenue North, Worcester, MA 01655. Uri.Galili@umassmed.edu.

Disclosures The authors have no financial conflicts of interest.

recruitment of macrophages into wounds and localized activation of these cells may accelerate healing.

Macrophages are physiologically recruited into wounds by chemotactic factors, such as MIP-1, MCP-1, and RANTES, released from cells within and around the wound and from endothelial cells at injury sites (8–12). Migration of macrophages into wounds can be markedly accelerated by exploiting the complement system. In many microbial infections, Ab interaction with Ags on the invading pathogen results in complement activation and formation of complement cleavage peptides, such as C5a and C3a. These complement cleavage peptides are effective chemotactic factors that direct extravasation of neutrophils and monocytes from blood vessels, differentiation of monocytes into macrophages, and migration of macrophages into infection sites (13, 14). We exploited this immune mechanism of complement activation for rapid recruitment and activation of macrophages by eliciting an Ag–Ab interaction within treated wounds. We hypothesized that topically applied liposomes with glycolipids that carry Galα1-3Galβ1-4GlcNAc-R epitopes (α-gal liposomes) would bind the natural anti-Gal Ab to generate Ag–Ab complexes that would activate the complement system, recruit and activate macrophages at the wound site, and promote wound healing.

Anti-Gal is the most abundant natural Ab in humans. It constitutes ~1% of serum Igs in all young and elderly individuals that are not severely immunocompromised (15, 16). Anti-Gal Ab production is elicited as a result of constant antigenic stimulation by gastrointestinal bacteria (17). Anti-Gal Ab interacts specifically with a carbohydrate Ag called the Galα1-3Galβ1-4GlcNAc-R (α-gal) epitope on glycolipids and glycoproteins (18, 19). This Ab is naturally produced in large amounts in humans, apes, and Old World monkeys, all of which have no α-gal epitopes because they lack the glycosylation enzyme α1,3galactosyltransferase (α1,3GT) (15, 18–20). In contrast, nonprimate mammals, prosimians, and New World monkeys synthesize α-gal epitopes by α1,3GT and lack anti-Gal Ab (19, 20). In vivo interaction between anti-Gal Ab and α-gal epitopes results in a very effective activation of the complement system. Such in vivo complement activation was demonstrated in xenotransplantation studies (21–25). Following xenotransplantation of pig organs into humans or monkeys, binding of serum anti-Gal Ab to the multiple α-gal epitopes on endothelial cells of pig xenografts activated complement, causing cytolysis of these cells, collapse of the vascular bed, and rapid (hyperacute) rejection (21–25).

We mimicked this process of localized complement activation by using α-gal liposomes structured to deliver very large numbers of α-gal epitopes (~10^{15} α-gal epitopes/mg liposomes) on their membranes. This amount is equivalent to that of α-gal epitopes present on 10^5 pig endothelial cells (20). When applied on wounds, α-gal liposomes introduce a very high concentration of α-gal epitopes into the treatment site. These multiple α-gal epitopes effectively bind anti-Gal Ab present in the fluid containing serum proteins leaking from damaged capillaries in the wound.

We hypothesized that this Ag–Ab interaction results in two consecutive processes that accelerate wound healing: first, anti-Gal/α-gal liposome interaction activates the complement system and generates chemotactic complement cleavage peptides (e.g., C5a and

C3a) that induce rapid migration of macrophages into the wound site. Second, the interaction between the Fc "tails" of anti-Gal Ab coating the α-gal liposomes and FcγRs on macrophages migrating into the wound activates the macrophages, similar to macrophage activation by various immune complexes (26). The activated macrophages produce cytokines that promote tissue repair. Combined, these two cellular processes should accelerate wound healing.

The interaction between anti-Gal in human serum and α-gal liposomes, leading to complement activation, can be readily demonstrated in vitro. However, experimental animal models, such as mice and other nonprimate mammals, synthesize α-gal epitopes and are unable to produce anti-Gal Abs because of immune tolerance to these self-epitopes (19, 20). Therefore, standard laboratory (wild-type) mice cannot be used as an animal model for anti-Gal–associated studies. A mouse lacking self α-gal epitopes has been generated by targeted disruption (i.e., knockout [KO]) of the α1,3GT gene (αGT KO) (27). This αGT KO mouse is not immunotolerant to α-gal epitopes and can produce anti-Gal Abs with characteristics similar to those of human anti-Gal Abs (27–32). In the current study, we used αGT KO mice with circulating anti-Gal Abs to document that treatment of wounds with α-gal liposomes induced rapid recruitment and activation of macrophages, accelerated healing of excisional wounds, and decreased scar formation.

Materials and Methods

Materials

Rabbit RBCs and pig kidneys were purchased from PelFreez (Rogers, AR). Pig RBCs from αGT KO pigs were a generous gift from Fios Therapeutics. Peroxidase (HRP)-coupled goat anti-mouse IgG and IgM Abs were purchased from Accurate Chemicals (Westbury, NY), HRP-coupled F4/80 anti-mouse macrophage Ab was purchased from Caltag (Invitrogen, MD), and rhodamine-coupled Abs for CD11b were purchased from Pharmingen (San Diego, CA). HRP-coupled rabbit anti-human IgG Abs were purchased from Dako (Copenhagen, Denmark). FITC-coupled *Bandeiraea* (*Griffonia*) *simplicifolia* IB4 lectin (BS lectin) was purchased from Vector Labs (Burlingame, CA). Cobra venom factor (CVF) was purchased from Sigma (St. Louis, MO).

Preparation of α-gal liposomes and nanoparticles used for wound dressing

α-Gal glycolipids make up the majority of glycolipids in rabbit RBCs (33–39). Therefore, α-gal liposomes were prepared from rabbit RBC membranes, as previously described (30, 40). Batches of 1 l rabbit RBCs were lysed in water and washed repeatedly to remove hemoglobin. For the extraction process, rabbit RBC membranes (RBC ghosts) were mixed with 1000 ml chloroform and 1000 ml methanol (1:1 chloroform/methanol) for 2 h and then 1000 ml methanol was added for overnight incubation with constant stirring (1:2 chloroform/methanol). The extract was filtered under vacuum through Whatman filter paper for removing residual RBC membranes and precipitated proteins. The membrane extract was dried in a rotary evaporator. Saline (20 ml) was added to the evaporation flask, and the dried extract was sonicated in a sonication bath to form liposomes. The liposome suspension was spun at 1,000 rpm for 10 min to remove precipitating materials that form a pellet.

Supernatants containing liposomes were further centrifuged at 14,000 rpm, and the liposome pellet volume was determined. The pellets were resuspended in the supernatant at a final concentration 100 mg/ml (10% v/v). The liposomes are referred to as α-gal liposomes, because they present an abundance of α-gal epitopes on their membranes.

Size evaluation using a microscope indicated that most α-gal liposomes were 0.5–3.0 μm. In some of the wound-healing studies, these liposomes were further converted into submicroscopic α-gal liposomes with an estimated diameter of 100–300 nm. Liposomes of this size range are referred to as nanoparticles. This decrease in liposome size was achieved by additional sonication using a sonication probe in a tube placed on ice within a laminar flow hood. The sonication was performed for 10 min, with the sonication probe intermittently active for 30 s in 30-s intervals. The determination that the sonicated α-gal liposomes have the size of nanoparticles is based on the finding that >90% of the particles passed through a 0.2-μm filter (Nalgen) and that >99% of the sonicated liposomes could not be visualized by light microscopy.

Preparation of control liposomes lacking α-gal epitopes

Control liposomes lacking α-gal epitopes were prepared from αGT KO pig RBCs. These αGT KO pigs lack α-gal epitopes because of targeted disruption (KO) of the α1,3GT gene (41). The αGT KO pig blood was received as a generous gift from Fios Therapeutics (Rochester, MN). Control αGT KO pig liposomes were prepared by a method identical to the one described above for α-gal liposomes.

Breeding and immunization of αGT KO mice

Mice used in this study have disrupted (KO) α1,3GT genes (27) and are referred to as αGT KO mice. The mice were generated on a C57BL/6 3 BALB/c genetic background and were bred and maintained at the animal facility of the University of Massachusetts Medical School. All experiments were performed with male and female mice. Study protocols were approved by the University of Massachusetts Institutional Animal Care and Use Committee and are in compliance with national guidelines. Anti-Gal Ab production was elicited in αGT KO mice by three or four weekly i.p. immunizations with 50 mg pig kidney membrane homogenate (i.e., xenogeneic membranes expressing multiple α-gal epitopes) (28–30). Production of anti-Gal Ab in αGT KO mice was confirmed to be at titers similar to those observed in humans (titers of 1:100–1:2000), by ELISA with synthetic α-gal epitopes linked to BSA (Dextra UK) as solid-phase Ag (28–30).

Treatment of excisional skin wounds with α-gal liposomes

Wounds were formed in shaved abdominal flanks of anesthetized αGT KO mice. A 3 × 6-mm oval skin incision was made in the right abdominal flank of the mouse. The epidermis, dermis, and upper part of the hypodermis were removed in the wound area created by this incision, resulting in the exposure of the connective tissue fascia over the panniculus carnosus muscle layer. Prior to treatment, 0.1 ml of the liposome suspension containing 10 mg α-gal liposomes was applied to the pad (1 × 1cm) of a small circular wound dressing (clear “spot” bandage; CVS Pharmacies) in a sterile laminar flow hood. The pads of the control wound dressings had 0.1 ml saline or 10 mg αGT KO pig liposomes applied. The

wound dressing was applied to cover the wound and was further covered with Tegaderm and with Transpore adhesive tape (3M, St. Paul, MN) to prevent removal by the mouse.

Preparation of peritoneal macrophages

αGT KO mice were injected i.p. with 1.5 ml of a 4% Brewer's thioglycolate solution. Macrophages migrating into the peritoneal cavity were harvested after 7 d by i.p. injection of 10 ml PBS into euthanized mice and subsequent collection of the fluid from the peritoneal cavity.

Flow cytometry analysis

Binding of anti-Gal Ab-coated α-gal liposomes via Fc–FcγR interaction in macrophages was measured by flow cytometry. α-Gal liposomes were coated with mouse anti-Gal IgG Abs by 1 h incubation with αGT KO mouse serum diluted 1:50. The liposomes (1 mg/ml) were washed and further incubated with mouse peritoneal macrophages for 1 h at 4°C. The cells were washed at 1000 rpm for removal of unbound liposomes and then stained with rhodamine anti-CD11b Ab (macrophage specific) and with FITC-BS lectin, which binds to α-gal epitopes on the liposomes. After 30 min of incubation, cells were washed, fixed, and subjected to flow cytometry analysis. Macrophages incubated with non–Ab-coated α-gal liposomes served as controls.

Analysis of the expression of cytokine genes associated with tissue healing

Activation of macrophage genes encoding for cytokines associated with healing was evaluated in αGT KO mouse skin 48 h postinjection with 10 mg α-gal liposomes, or with αGT KO pig liposomes lacking α-gal epitopes. Gene activation in the injected skin was determined by quantitative real-time PCR (q-RT-PCR). Skin specimens from mice injected with saline served as controls. Custom-made SABiosciences (Frederic, MD) q-RTPCR 96-well plates containing primers for 11-cytokine encoding genes and for the housekeeping gene *GADPH* were used for this purpose. The reaction was performed with SYBR Green master mix solution (SABio-sciences PA-011). Expression of the following genes was measured: Fgf1, Il1a, IL6, Pdgfb, Tnf, Vegfa, Bmp2, Fgf2, Csf1, and *Csf2*. Total RNA was isolated using gentle MACS (Miltenyi Extractor apparatus), followed by mRNA isolation and cDNA synthesis using Miltenyi Magnetic Micro Beads. The cDNA was added as ~1 ng/well to wells containing the various primers. PCR reaction (30 cycles) was performed in the Biorad MyiQ single-color Real Time PCR detection system. The results were normalized based on the housekeeping gene and fold increase in C_t values (threshold concentration) determined by using the software program provided on the SABioscience Web site that calculates $\Delta\Delta C_t$-based fold change.

Analysis of in vitro secretion of vascular endothelial growth factor by macrophages

Macrophages coincubated with anti-Gal–coated α-gal liposomes or with α-gal liposomes not coated by anti-Gal Ab were plated in 24-well plates at 3×10^5 cells/well in 1 ml volume. Macrophages cultured without liposomes served as control. Supernatants were collected after 24 and 48 h and subjected to analysis of vascular endothelial growth factor (VEGF)

secretion using a VEGF ELISA kit (Antigenix, NY), according to the manufacturer's protocol.

ELISA with liposomes as solid-phase Ag

Binding of anti-Gal IgG in αGT KO mouse sera to α-gal liposomes and to αGT KO pig liposomes was studied in ELISA wells that were coated with these liposomes. Liposomes in PBS (1 mg/ml) were dried in ELISA wells, resulting in firm attachment of the liposomes to the wells. After blocking with PBS containing 1% BSA, αGT KO mouse serum samples at serial 2-fold dilutions were placed as 50-μl aliquots in liposome-coated wells and incubated for 2 h at 24°C. The wells were washed with PBS containing 0.05% Tween, and HRP-coupled anti-mouse IgG Abs were added for 1 h. Color reaction was developed with *o*-phenylenediamine, and absorbance was measured at 492 nm.

Histological analysis

Wound healing was determined in histological sections and expressed as the percentage of wound surface covered with regenerating epidermis. The wound bed was determined by the intact dermis. The number of infiltrating neutrophils and macrophages at skin sites injected with liposomes was determined by counting cells within a rectangular area demarcated in a microscope lens at ×400 magnification. The rectangle, with a size corresponding to 100 × 200 μm at that magnification, was placed at the border of the liposome hypodermic injection site within the skin. Neutrophils were identified by segmented nuclei, and macrophages were identified by the kidney- or oval-shaped nuclei and large size of the cells. Four fields were counted in each section. Two sections of the same specimen were evaluated. The data represent mean + SD from at least five mice/group.

Statistics

An ANOVA test was used for statistical analyses. A p value < 0.05 was considered statistically significant.

Results

In vitro interaction of anti-Gal–coated α-gal liposomes with αGT KO mouse macrophages induces VEGF secretion

We first generated α-gal liposomes using rabbit RBCs that provide multiple glycolipids with α-gal epitopes (α-gal glycolipids). As we showed previously, incubation of rabbit RBC membranes with chloroform and methanol results in extraction of phospholipids, cholesterol, and multiple α-gal glycolipids (33). Rabbit RBCs have the highest concentration of α-gal glycolipids among mammals, ranging in chain size from 5–40 carbohydrates, and having one, two, or multiple branches, each capped with an α-gal epitope (34–39). Sonication of the dried organic extract from rabbit RBC membranes in saline results in formation of liposomes constructed of a membrane of phospholipids and cholesterol and multiple α-gal glycolipids anchored in that membrane (30, 40). Because of the many α-gal epitopes on these liposomes (~10^{15} α-gal epitopes/mg liposomes), they have been designated α-gal liposomes and were found to interact effectively with anti-Gal produced by αGT KO mice (30, 40).

We first studied the ability of anti-Gal/α-gal liposomes to interact with αGT KO mouse macrophages and activate them. Such activation was documented by measuring VEGF secretion. For these experiments, α-gal liposomes precoated with αGT KO mouse anti-Gal Abs were incubated with αGT KO mouse peritoneal macrophages. Non–Ab-coated α-gal liposomes incubated with macrophages served as controls. Binding of liposomes to macrophages was determined by flow cytometry following double staining of fluorescein (green)-coupled BS lectin binding specifically to α-gal epitopes (18, 19)] and rhodamine (red)-coupled anti-CD11b Ab (specific for macrophages).

Non–Ab-coated α-gal liposomes adhered to ~15% of the macrophages (Fig. 1*A*). However, binding increased by ~4-fold when the liposomes were coated with anti-Gal Ab (55%) (Fig. 1*B*). These data are similar to those observed using a system in which tumor cells coated with mouse or human anti-Gal Abs bound to mouse and human macrophages via Fc–FcγR interaction (31, 32).

VEGF secretion was quantified in peritoneal macrophages cocultured with anti-Gal–coated or non–Ab-coated α-gal liposomes to determine whether macrophages were activated by the anti-Gal/α-gal liposome immune complexes. Macrophages cocultured with anti-Gal–coated α-gal liposomes produced 2–4-fold more VEGF than did the same macrophages incubated with α-gal liposomes lacking anti-Gal Ab (Fig. 1*C*). The latter macrophages produced low levels of VEGF, similar to those secreted by macrophages cultured in the absence of liposomes. These findings support the assumption that interaction between the Fc portion of anti-Gal Ab bound to α-gal liposomes and FcγR on macrophages activates these cells to produce and secrete tissue-healing cytokines.

Recruitment of macrophages into skin sites injected with α-gal liposomes

Studies on the in vivo interaction between anti-Gal Abs with α-gal liposomes require animal models that lack self-expressed α-gal epitopes and can generate anti-Gal Abs. The αGT KO mouse lacks α-gal epitopes (27). Following immunization with pig kidney membranes, these mice produce anti-Gal Abs in titers comparable to those attained in humans (28–30). Anti-Gal produced in the immunized mice displays characteristics (i.e., classes and subclasses) similar to human anti-Gal Abs (29). Anti-Gal Abs produced in αGT KO mice can readily bind to α-gal liposomes (30, 40).

The effect of anti-Gal/α-gal liposome interaction on localized recruitment of macrophages was studied in vivo in anti-Gal Ab-producing αGT KO mice injected s.c. with 10 mg α-gal liposomes in 0.1 ml saline. Control liposomes were generated using αGT KO pig RBCs that lack α-gal epitopes due to targeted disruption of the α1,3GT gene (41). As with αGT KO mice, αGT KO pigs completely lack α-gal glycolipids; therefore, liposomes produced from their RBC membranes completely lack α-gal epitopes. Because αGT KO pig liposomes lack α-gal epitopes, they do not bind IgG Abs in αGT KO mouse serum, as indicated in ELISA in wells coated with αGT KO pig liposomes (Fig. 2). The marginal binding of IgG Abs at the lowest dilutions is likely to be nonspecific binding of serum IgG to the ELISA wells. In contrast, anti-Gal in these sera readily binds to α-gal liposomes coating ELISA wells (Fig. 2). This binding is detectable (>1.0 OD) even at serum dilutions of 1:320, whereas no such binding was observed at the lowest dilution (1:20) in wells coated with αGT KO pig

liposomes. Previous studies by flow cytometry demonstrated a similar interaction of anti-Gal IgG and IgM Abs with α-gal liposomes incubated in αGT KO mouse serum (40).

Skin specimens were obtained from euthanized mice at various time points, fixed, and stained with H&E (Fig. 3). The empty areas in Fig. 3*A*, 3*F*, and 3*G* are likely injection sites where liposomes were dissolved by ethanol and removed during the staining process. Within 12 h, the injection site in the hypodermis was surrounded by neutrophils (Fig. 3*A*, 3*D*). Most of the neutrophils had disappeared by 24 h and were replaced by infiltrating macrophages (Figs. 3*B*, 3*E*, 4). These infiltrating cells were confirmed to be macrophages by anti-macrophage Ab (F4/80 Ab) immunostaining, 96 h post α-gal liposome injection (Fig. 3*K*). Macrophage recruitment seems to be highly dependent on activation of the complement cascade. This is suggested from the low macrophage recruitment observed 24 h after coinjection of α-gal liposomes and CVF (20 μg), which inhibits complement activation (Figs. 3*C*, 4). The significance of α-gal epitope expression on liposomes for induction of rapid recruitment of macrophages through complement activation is further strengthened by failure of 10 mg αGT KO pig liposomes (liposomes lacking α-gal epitopes) to induce recruitment within 24 h postinjection (Figs. 3*F*, 4).

Inspection of α-gal liposome injection sites after 4 and 7 d (Fig. 3*K*, 3*J*, respectively) revealed a gradual increase in the size of macrophages and the formation of large clusters of these cells with almost no space between the macrophages. Individual macrophages inspected after 7 d were very large (20–30 μm) and contained multiple vacuoles that represented the internalized α-gal liposomes (Fig. 3*L*). This morphology of infiltrating macrophages was also observed 14 d postinjection (Fig. 3*H*). However, by 4 wk, all macrophages had disappeared, and the injected skin displayed normal histology, with no indication of a localized long-term immune response (Fig. 3*I*). Parallel studies in mice injected s.c. with saline did not show evidence of recruitment of cells into the injection site at any time point (data not shown).

In vivo induction of cytokine gene expression by injected α-gal liposomes

In vitro studies of macrophages that interact with α-gal liposomes (Fig. 1) suggested that these cells were activated following the Fc–FcγR interaction with anti-Gal Ab coating these liposomes. We next determined whether macrophages migrating into the injection sites of α-gal liposomes activate genes encoding cytokines that promote wound healing. To test this, αGT KO mice were injected s.c. with 10 mg α-gal liposomes (Figs. 3, 4) or with saline as control. After 48 h, the skin at the injection site was harvested, RNA was extracted, mRNA was isolated, and cDNA was synthesized and subjected to q-RT-PCR with primers specific for 11 cytokine genes known to be produced by activated macrophages. GADPH was used as a control housekeeping gene for normalizing the cDNA. Skin specimens from αGT KO mice injected with αGT KO pig liposomes served as a specificity control for the effect of liposomes that lack α-gal epitopes. Because of variations in extracted mRNA, the data were normalized to the housekeeping GAPDH expression using the SABiosciences software program. The extent of gene expression was calculated and presented as relative fold change compared with saline-injected skin specimens (Fig. 5).

Although there was a mouse to mouse variation, three of the assayed genes (*Il1a*, *Pdgfb*, and *Csf1*) displayed ≥3-fold increase in expression compared with controls and expression that was significantly higher than that in the skin of αGT KO mice injected with liposomes lacking α-gal epitopes (i.e., liposomes prepared from αGT KO pig RBCs) (Fig. 5). Activation of the genes for cytokines that promote wound healing in mice injected with α-gal liposomes (Fig. 5) coincided with the observed extensive recruitment of macrophages into the injection site (Fig. 4). These data strongly suggested that these activated genes are expressed in macrophages recruited by anti-Gal/α-gal liposome interaction.

α-Gal liposome treatment accelerates epidermal healing of skin wounds

The above observations on accelerated recruitment of macrophages and activation of these cells following ant-Gal/α-gal liposome interaction suggested that topical application of these liposomes on wounds might induce accelerated healing. To test this, we performed excisional skin wounds (~3 × 6-mm oval excision) in which epidermis, dermis, and the upper part of the hypodermis were removed from the abdominal flank of anesthetized αGT KO mice. The wounds were treated with 10 mg α-gal liposomes, 10 mg αGT KO pig liposomes (lacking α-gal epitopes), or saline on a 10 × 10-mm pad of spot bandages used as wound dressing. The gross appearance of the wound was documented on various days, and the wound area was removed from euthanized mice and subjected to histological analysis. Wound healing was determined by the percentage of wound surface covered by regenerating epidermis. This was evaluated by histological analysis (Figs. 6–8), as well as by morphology on day 6 in cohorts of mice (Fig. 9).

Control wounds treated for 3 d with dressing that had saline displayed no evidence of regeneration of the epidermis (Fig. 6) and no significant infiltration of macrophages into the wound (Fig. 7A). In contrast, wounds treated with α-gal liposomes for 3 d displayed extensive infiltration of mononuclear cells with macrophage morphology and that formed a characteristic granulation tissue (Fig. 7*B*). These α-gal liposome-treated wounds also exhibited a distinct initiation of epidermis regeneration, as indicated by the multilayered large epidermal cells observed over the newly formed dermis at the border of the injured area (Figs. 6, 7*B*). The regenerating epidermis covered, on average, 12% of the wound (Fig. 6). Control wounds treated with αGT KO pig liposomes displayed only residual epidermis regeneration (Fig. 6).

By day 6, control saline-treated wounds displayed extensive infiltration of macrophages into the regenerating dermis (Fig. 7*C*, 7*E*) and initial regeneration of the epidermis (Fig. 7*E*). However, at this time point, the regeneration of the epidermis was observed only at the periphery of the wound, whereas the dermis remained exposed at the center of the wound (Fig. 7*C*). The leading edge of the regenerating epidermis on day 6 in saline-treated wounds is shown in Fig. 7*E*. In wounds treated for 6 d with saline, the regenerating epidermis covered only ~20% of the wound surface (Fig. 6). Wounds treated with αGT KO pig liposomes also displayed ~20% healing on day 6. In contrast, the extent of epidermis regeneration in wounds treated with α-gal liposomes was much higher on day 6 and reached an average of ~60% of the wound surface (Figs. 6, 9). At this time, ~35% of mice treated with α-gal liposomes displayed complete closure of the wound by regenerating epidermis

(Fig. 7). In the remaining mice, the regenerating epidermis covered 30–80% of the wound (Fig. 9). This regenerating epidermis is thicker than regular epidermis (four to eight layers of epithelial cells versus two layers, respectively), suggesting a highly proliferative state of epidermal cells (Fig. 7*D*, 7*F*). Also, in many α-gal liposome-treated wounds examined on day 6 the dermis was thicker than that in saline-treated wounds (Fig. 7*D* versus 7*C*), suggesting accelerated regeneration of the dermis. By day 9, only ~40% of the surface of saline- or αGT KO pig liposome-treated wounds was covered by regenerating epidermis (Fig. 6). In comparison, most α-gal liposome-treated wounds showed complete epidermal closure, with some displaying 60–90% regeneration. However, variations in the extent of healing were observed between animals, and the SD at various time points, particularly in the α-gal liposome-treated wounds, is high (Fig. 6).

After 12 d of treatment, on average, ~60% of the wound surface in saline- and αGT KO pig liposome-treated wounds were covered by the regenerating epidermis, whereas most of the α-gal liposome-treated wounds were completely covered by epidermis. Overall, the regeneration of epidermis in wounds treated with α-gal liposomes was approximately twice as fast as the physiologic regeneration of saline-treated wounds (Fig. 6). The similar rate of epidermis regeneration in saline-treated and αGT KO pig liposome-treated wounds strongly suggested that accelerated regeneration in these studies is dependent on α-gal epitope presentation on the liposomes.

The efficacy of α-gal liposomes in inducing accelerated healing was further increased by reducing their size. These liposomes were converted into α-gal nanoparticles by sonication. Application of 10 mg α-gal nanoparticles on wounds resulted in regeneration of ~40% of the wound epidermis within 3 d (Fig. 6). By day 6, 60% of the treated wounds displayed complete regeneration of the epidermis, whereas the remaining 40% displayed 95% epidermis regeneration (Figs. 6, 9). As controls, we observed that healing following treatment with αGT KO pig nanoparticles did not differ from that observed using αGT KO pig liposomes (data not shown).

The differences in efficacy between α-gal nanoparticles and α-gal liposomes may be attributed to the fact that there are many more particles in 10 mg of α-gal nanoparticles than in 10 mg of α-gal liposomes. This is because each liposome is split by sonication into several nanoparticles. Thus, it is possible that α-gal nanoparticles diffuse better than α-gal liposomes throughout the wound as a result of their higher number and smaller size. Increased diffusion would likely result in increased efficacy of recruitment and activation of macrophages.

Regeneration of dermis in wounds as evaluated by trichrome staining

Evaluation of connective tissue (i.e., dermis and hypodermis) regeneration in the wound can best be performed following trichrome staining. The collagen fibers of the connective tissue within the dermis and hypodermis are stained blue, whereas epidermal- and dermal-residing cells are stained purple (Fig. 8). Although α-gal liposome-treated wounds displayed regenerating dermis within 3 d of wounding (Fig. 8*B*), no evidence for regeneration was observed in the saline-treated wounds (Fig. 8*A*). In the α-gal liposome-treated wounds, initiation of dermal recovery was indicated by the collagen fibers appearing beneath the

regenerating epidermis (Fig. 8*B*). The uninjured dermis surrounding the wound was characterized by deep blue staining of collagen that was much denser than the newly formed collagen in the regenerating dermis. The histology presented in Fig. 8*B* suggested that collagen-secreting fibroblasts are among the first cells recruited within 72 h postinjury into wounds treated with α-gal liposomes.

Day-6 control wounds showed newly formed dermis that contained multiple macrophages (Fig. 8*C*, 8*E*). A distinct border is present between the newly formed dermis and the uninjured dermis in day-6 control wounds (Fig. 8*E*). Newly formed dermis filled with many cells was also observed on day 6 in wounds treated with α-gal liposomes (Fig. 8*D*, 8*F*). Some of the cells residing in the regenerating dermis are fibroblasts depositing collagen. Many of the other cells forming the granulation tissue in this dermis are likely to be macrophages that have been recruited into the wound.

α-Gal liposome treatment reduces scar formation

To investigate whether accelerated healing of wounds by α-gal liposomes could result in hyperplasia of the epidermis and/or scar formation, wounds were subjected to histological analysis 28 d postwounding and treatment. Control wounds treated for 28 d with saline-coated dressing displayed wide areas of dense dermis devoid of skin appendages, characteristic of scar formation. In addition, the regenerating epidermis in these control wounds was thicker than normal epidermis and had at least five layers of cells (Fig. 10*A–D*). The histology of wounds treated with αKO pig liposomes was similar to that of wounds treated with saline (Fig. 10*E–H*). This scar formation is a reflection of the physiologic default mechanism for filling the injured area with dense connective tissue and with epidermis that is thicker than in uninjured skin. In contrast, epidermis in α-gal liposome-treated wounds displayed normal thickness of two cell layers, and the density of collagen in the dermis, based on trichrome staining, was normal (Fig. 10*I–L*). Healed wounds treated with α-gal liposomes also contained regenerating appendages, such as hair follicles and sebaceous glands, as well as fat cells. A similar regeneration without scar formation was observed in wounds treated with α-gal nanoparticles (data not shown). It is notable that all treated wounds contained no granuloma at 28 d and that most macrophages had disappeared from the wounds at that time point (Fig. 10).

Overall, these findings suggested that the healing of wounds without formation of a scar requires the rapid recruitment of macrophages and their effective activation due to anti-Gal Ab interaction with α-gal liposomes or nanoparticles. In the absence of such interaction, as with KO pig liposomes lacking α-gal epitopes, healing results in scar formation similar to that observed in physiologic healing in saline-treated wounds.

Discussion

This study describes a novel method for inducing rapid recruitment and activation of macrophages by α-gal liposomes and by α-gal liposomes sonicated into nanoparticles, both interacting with natural anti-Gal Abs. This recruitment and activation of macrophages accelerate wound healing in αGT KO mice while avoiding scar formation. Because humans naturally produce anti-Gal Abs that constitute ~1% of IgG, IgM, and IgA Igs in their serum

(15, 42–44), topical application of α-gal liposomes may also result in accelerated wound healing in a clinical setting.

Very large amounts of α-gal epitopes on glycolipids of α-gal liposomes bound anti-Gal Abs and induced strong complement activation. Because there are ~10^{15} α-gal epitopes/mg liposomes, their topical application on wounds results in a high concentration of α-gal epitopes on the wound surface, allowing for robust local interaction with anti-Gal Abs released from damaged capillaries and the ensuing local activation of the complement cascade. The diminished recruitment of macrophages following injection of CVF, together with α-gal liposomes, suggests the need for complement activation but does not prove it. The direct activation of complement by anti-Gal–binding α-gal glycolipids was demonstrated in a previous study (33). It is difficult to demonstrate such direct activation by anti-Gal/α-gal liposome interaction in treated wounds because the activated complement is deposited on α-agal liposomes following anti-Gal binding. These liposomes are washed from wound specimens during processing for histological evaluation and are dissolved in the alcohol used for fixation.

Liposomes that do not express α-gal epitopes have been used in wound healing as vesicles for delivery of substances to wounds that affect wound healing, such as superoxide dismutase (45) and hemoglobin (46), or of genes that encode growth factors (47). The α-gal liposomes deliver multiple α-gal glycolipids in their membranes, rather than within the liposomes, to mediate their therapeutic effects. Our data showed that the novel aspects in α-gal liposome treatment versus other wound-healing treatments are the harnessing of at least two immunological mechanisms for accelerating the healing process. First, anti-Gal/α-gal liposome interaction activates complement to produce complement cleavage peptides that induce rapid extravasation of monocytes, their conversion into macrophages, and their chemotactic migration into the treated wound. Second, Fc–FcγR interaction between anti-Gal–coated α-gal liposomes and recruited macrophages results in activation of these cells and secretion of cytokines that promote wound healing.

This study suggests that the macrophages recruited following anti-Gal/α-gal liposome interaction were activated, resulting in production of various cytokines. Increased specific expression of *Il1a, Pdgfb,* and *Csf1* further suggests that these genes may be involved in wound healing. We also observed that anti-Gal–coated α-gal liposomes activated macrophages to secrete VEGF in vitro, but we were unable to confirm this in vivo. Elevated cytokine gene activity in macrophages is usually observed in inflammation. It may be possible that after an initial proinflammatory response, the macrophages start to secrete healing-promoting (prohealing) cytokines or they recruit macrophages that produce cytokines that promote the repair of the injured tissue. In our study, the analysis of cytokine gene expression was performed 48 h postintradermal injection of α-gal liposomes. It is not clear whether the observed elevated cytokine activity at that early stage is already associated with the prohealing activity of macrophages. Detailed correlation between the various stages of the wound-healing process (evaluated by histology and immunostaining) and the expression level of various cytokine genes will allow for establishing the association between temporal changes in cytokine gene expression and the resulting histological effects, as previously demonstrated (48). Such analysis will enable the comparison of these

parameters between α-gal liposome-treated wounds and wounds that undergo physiologic healing.

The direct mechanisms contributing to the in vivo activation of macrophages and the subsequent activation of the cytokine genes by anti-Gal–coated α-gal liposomes were not evaluated in the current study. The increased binding of anti-Gal–coated α-gal liposomes to mouse macrophages, the increased VEGF production following this interaction, and the previously demonstrated interaction of human immunocomplexed anti-Gal with FcγR on autologous macrophages (32) suggest that a similar Fc–FcγR interaction is likely to occur in vivo between anti-Gal on α-gal liposomes and human macrophages. However, additional studies are required to determine whether activation of macrophages as a result of this Fc–FcγR interaction is similar to the interaction of other immune complexes with FcγRs on macrophages (26).

The ultimate result of the rapid recruitment of macrophages and their activation by anti-Gal/α-gal liposome immune complexes is the accelerated healing of wounds. By comparing the extent of epidermis regeneration in α-gal liposome-treated wounds to that in control wounds, this treatment seems to decrease the mean healing time by ~50%. The histological observation of macrophages in the α-gal liposome-treated wounds at 72 h was associated with efficient regeneration of epidermis on day 6, suggesting that anti-Gal/α-gal liposome interaction induces the rapid recruitment of macrophages and the activation of these cells to produce cytokines that mediate wound healing. These observations are supported by studies on healing of skin burns treated with α-gal liposomes, which also demonstrated ~50% decrease in healing time due to accelerated recruitment and activation of macrophages by anti-Gal Ab bound to α-gal liposomes (40). The efficacy of this wound-healing process was improved by decreasing the α-gal liposome size to that characteristic of nanoparticles. This was achieved by additional sonication of the liposomes. This sonication splits liposomes into submicroscopic liposomes referred to as α-gal nanoparticles. Treatment of wounds with α-gal nanoparticles decreased the wound healing time by ~70%, resulting in complete regeneration of the epidermis in the majority of mice within 6 d of treatment. It is possible that the larger number of submicroscopic particles generated by splitting of each liposome and the increased diffusion of these multiple nanoparticles throughout the wound contribute to a faster recruitment and more effective activation of macrophages in treated wounds.

The early increased production of healing-promoting cytokines by activated macrophages may also be associated with the observed lack of hyperplasia in skin tissues and the decrease in scar formation. Such a decrease in scar formation was demonstrated in healing wounds in αGT KO mice treated with α-gal liposomes but not in those treated with saline or with KO pig liposomes (liposomes lacking α-gal epitopes). Formation of scar tissue (i.e., dense connective tissue lacking skin appendages and covered with thick epidermis) is the physiologic default mechanism for wound healing that occurs after the closure of the wound with regenerating epidermis. We suggest that rapid anti-Gal–mediated activation of recruited macrophages to secrete cytokines that promote tissue healing may lead to restoration of the cellular components of normal skin, prior to the scar-formation process. Proving this will require a larger and more long-term study. Nevertheless, the histology of day-28 wounds

strongly suggested that α-gal liposome treatment did not induce hyperplasia and formation of scars in the skin tissues during the healing process.

Activation of macrophages in wounds was demonstrated by application of immunomodulating substances, such as carrageenan (49) and BCG (50). However, these treatments also resulted in nonbeneficial prolonged inflammatory immune responses that may be manifested as chronic granulomas (49, 50). No chronic granuloma formation was observed in wounds 1 mo after the initiation of α-gal liposome or α-gal nanoparticle treatment. This implies that the rapid recruitment and activation of macrophages is not followed by any additional immune response to the treating substance. This is likely to be associated with the lack of immunogenicity of α-gal liposomes, which contain no antigenic proteins capable of activating T cells (28, 51). The α-gal epitope itself, like other Ags composed of carbohydrate chains of the complex type (e.g., blood group A and B Ags), does not activate T cells. In the absence of T cell help, the α-gal epitope does not elicit a B cell immune response (51). Moreover, the interaction between FcγR on the recruited macrophages and anti-Gal coating the α-gal liposomes results in the rapid internalization of these liposomes because of effective phagocytosis and their elimination from the wound. Following the removal of liposomes, the recruited macrophages disappear within 3–4 wk and do not elicit a chronic immune response or a granuloma within the treated wound. This restoration of normal skin histology 3–4 wk post-injection of α-gal liposomes and the diminished scar formation in α-gal liposome-treated wounds suggested that this treatment does not induce an overly exuberant inflammatory response that may be detrimental.

Treatment with α-gal liposomes in the clinical setting is of potential significance. If this treatment is found to be successful in humans, the resulting decrease in the healing time of wounds will reduce morbidity and decrease the costs associated with acute and chronic wound treatment, which are expected to increase significantly in the coming years (52). The following observations suggest that the accelerated wound healing in αGT KO mice may also be observed in patients with wounds treated with α-gal liposomes. First, anti-Gal Abs are present in very large amounts in all humans who are not severely immunocompromised. Second, anti-Gal Abs in human serum effectively bind to α-gal liposomes and induce complement activation. Third, human anti-Gal Abs immunocomplexed with α-gal epitopes readily bind to FcγR on macrophages (21, 32). Fourth, cultured human macrophages activated in vitro by hypotonic shock were found to accelerate wound healing in patients with deep sternal wounds (53) and with ulcers (7). The use of α-gal liposomes on wound dressings is likely to be much easier to perform than injection of activated macrophages into wounds because it does not require specialized equipment and facilities for in vitro culturing of macrophages. It is also possible that the treatment with α-gal liposomes in humans may be even more effective than that described above in αGT KO mice, because complement activity in human serum is many fold higher than that in mouse serum (33). In addition, because anti-Gal is present in all individuals who are not severely immunocompromised, including diabetic patients (54) and elderly individuals (16), the effective recruitment and activation of macrophages by α-gal liposomes may jumpstart the healing process in chronic wounds of diabetic patients and elderly individuals who usually display impaired wound healing. Because anti-Gal activity may vary from one person to another (55), it remains to be determined in clinical trials whether there is a correlation between the Ab activity and

rate of healing or whether Ab levels in all treated individuals are above a threshold level required for inducing accelerated healing.

α-Gal liposomes/nanoparticles are highly stable, and their α-gal epitopes do not alter their structure during prolonged storage. α-Gal epitopes, in contrast to biologically active proteins, have no folding or tertiary structures, leading to their robust stability. Furthermore, α-gal epitopes do not undergo oxidation for prolonged periods and can be stored for years without losing activity. This conclusion can be inferred from studies on blood group Ags. The structure of the α-gal epitope is very similar to that of blood group A and B Ags (18, 56). Because of their stability, these blood group Ags have been detected and characterized in Egyptian mummies that are >2000 y old (57). Thus, if α-gal liposomes/nanoparticles are found to be effective in accelerating wound healing in humans, they can be stored for prolonged periods and delivered to wounds in many forms, including sprays, hydrogels, on wound dressings, in suspension, or incorporated into devices and dressings that are currently used for treating injuries. Moreover, because repair and regeneration of internal injured tissues are also dependent on effective local recruitment and activation of macrophages (5), it is possible that delivery of α-gal liposomes/nanoparticles to such injuries (e.g., ischemic tissue and trauma injuries) may result in the accelerated regeneration and restoration of the original biological activity of the injured tissue, while avoiding irreversible scar formation.

Acknowledgments

We thank Drs. John Logan and Barry Wiseman of Fios Therapeutics for the generous gift of blood from α1,3GT KO pigs.

This work was supported in part by National Institutes of Health Grants CA122019 (to U.G.), CA66644 (to E.S.-T), and AI46629 (to D.L.G.) and Diabetes Endocrinology Research Center Grant DK32520 (to D.L.G.).

Abbreviations used in this article

anti-Gal	an Ab that binds specifically to Galα1-3Galβ1-4GlcNAc-R epitopes
BS lectin	*Bandeiraea* (*Griffonia*) *simplicifolia* IB4 lectin
CVF	cobra venom factor
α-gal	Galα1-3Galβ1-4GlcNAc-R
α-gal liposome	liposome with glycolipids that carry Galα1-3Galβ1-4GlcNAc-R epitopes
α1,3GT	α1,3galactosyltransferase
αGT KO	α1,3galactosyltransferase gene knockout
KO	knockout
q-RT-PCR	quantitative real-time PCR
VEGF	vascular endothelial growth factor

References

1. Leibovich SJ, Ross R. The role of the macrophage in wound repair. A study with hydrocortisone and antimacrophage serum. Am. J. Pathol. 1975; 78:71–100. [PubMed: 1109560]
2. DiPietro LA. Wound healing: the role of the macrophage and other immune cells. Shock. 1995; 4:233–240. [PubMed: 8564549]
3. Singer AJ, Clark RA. Cutaneous wound healing. N. Engl. J. Med. 1999; 341:738–746. [PubMed: 10471461]
4. Martin P. Wound healing—aiming for perfect skin regeneration. Science. 1997; 276:75–81. [PubMed: 9082989]
5. Duffield JS, Forbes SJ, Constandinou CM, Clay S, Partolina M, Vuthoori S, Wu S, Lang R, Iredale JP. Selective depletion of macrophages reveals distinct, opposing roles during liver injury and repair. J. Clin. Invest. 2005; 115:56–65. [PubMed: 15630444]
6. Daley JM, Brancato SK, Thomay AA, Reichner JS, Albina JE. The phenotype of murine wound macrophages. J. Leukoc. Biol. 2010; 87:59–67. [PubMed: 20052800]
7. Danon D, Madjar J, Edinov E, Knyszynski A, Brill S, Diamantshtein L, Shinar E. Treatment of human ulcers by application of macrophages prepared from a blood unit. Exp. Gerontol. 1997; 32:633–641. [PubMed: 9785089]
8. Piccolo MT, Wang Y, Sannomiya P, Piccolo NS, Piccolo MS, Hugli TE, Ward PA, Till GO. Chemotactic mediator requirements in lung injury following skin burns in rats. Exp. Mol. Pathol. 1999; 66:220–226. [PubMed: 10486240]
9. Heinrich SA, Messingham KA, Gregory MS, Colantoni A, Ferreira AM, Dipietro LA, Kovacs EJ. Elevated monocyte chemoattractant protein-1 levels following thermal injury precede monocyte recruitment to the wound site and are controlled, in part, by tumor necrosis factor-alpha. Wound Repair Regen. 2003; 11:110–119. [PubMed: 12631298]
10. Shukaliak JA, Dorovini-Zis K. Expression of the beta-chemokines RANTES and MIP-1 beta by human brain microvessel endothelial cells in primary culture. J. Neuropathol. Exp. Neurol. 2000; 59:339–352. [PubMed: 10888363]
11. Franz MG, Steed DL, Robson MC. Optimizing healing of the acute wound by minimizing complications. Curr. Probl. Surg. 2007; 44:691–763. [PubMed: 18036992]
12. Shallo H, Plackett TP, Heinrich SA, Kovacs EJ. Monocyte chemoattractant protein-1 (MCP-1) and macrophage infiltration into the skin after burn injury in aged mice. Burns. 2003; 29:641–647. [PubMed: 14556721]
13. Snyderman R, Pike MC. Chemoattractant receptors on phagocytic cells. Annu. Rev. Immunol. 1984; 2:257–281. [PubMed: 6100474]
14. Haeney MR. The role of the complement cascade in sepsis. J. Anti-microb. Chemother. 1998; 41(Suppl. A):41–46.
15. Galili U, Rachmilewitz EA, Peleg A, Flechner I. A unique natural human IgG antibody with anti-α-galactosyl specificity. J. Exp. Med. 1984; 160:1519–1531. [PubMed: 6491603]
16. Wang L, Anaraki F, Henion TR, Galili U. Variations in activity of the human natural anti-Gal antibody in young and elderly populations. J. Gerontol. A Biol. Sci. Med. Sci. 1995; 50:M227–M233. [PubMed: 7542151]
17. Galili U, Mandrell RE, Hamadeh RM, Shohet SB, Griffiss JM. Interaction between human natural anti-α-galactosyl immunoglobulin G and bacteria of the human flora. Infect. Immun. 1988; 56:1730–1737. [PubMed: 3290105]
18. Galili U, Macher BA, Buehler J, Shohet SB. Human natural anti-α-galactosyl IgG. II. The specific recognition of a (1-3)-linked galactose residues. J. Exp. Med. 1985; 162:573–582. [PubMed: 2410529]
19. Galili U, Clark MR, Shohet SB, Buehler J, Macher BA. Evolutionary relationship between the natural anti-Gal antibody and the Gala1-3Gal epitope in primates. Proc. Natl. Acad. Sci. USA. 1987; 84:1369–1373. [PubMed: 2434954]
20. Galili U, Shohet SB, Kobrin E, Stults CLM, Macher BA. Man, apes, and Old World monkeys differ from other mammals in the expression of α-galactosyl epitopes on nucleated cells. J. Biol. Chem. 1988; 263:17755–17762. [PubMed: 2460463]

21. Galili U. Interaction of the natural anti-Gal antibody with α-galactosyl epitopes: a major obstacle for xenotransplantation in humans. Immunol. Today. 1993; 14:480–482. [PubMed: 7506033]
22. Good H, Cooper DKC, Malcolm AJK, Ippolito RM, Koren E, Neethling FA, Ye Y, Zuhdi N, Lamontagne LR. Identification of carbohydrate structures that bind human antiporcine antibodies: implications for discordant xenografting grafting in man. Transplant. Proc. 1992; 24:559–562. [PubMed: 1566430]
23. Sandrin MS, Vaughan HA, Dabkowski PL, McKenzie IFC. Anti-pig IgM antibodies in human serum react predominantly with Gal(α1-3)Gal epitopes. Proc. Natl. Acad. Sci. USA. 1993; 90:11391–11395. [PubMed: 7504304]
24. Collins BH, Cotterell AH, McCurry KR, Alvarado CG, Magee JC, Parker W, Platt JL. Cardiac xenografts between primate species provide evidence for the importance of the α-galactosyl determinant in hyper-acute rejection. J. Immunol. 1995; 154:5500–5510. [PubMed: 7537308]
25. Sachs DH, Sykes M, Robson SC, Cooper DK. Xenotransplantation. Adv. Immunol. 2001; 79:129–223. [PubMed: 11680007]
26. Ravetch JV, Bolland S. IgG Fc receptors. Annu. Rev. Immunol. 2001; 19:275–290. [PubMed: 11244038]
27. Thall AD, Malý P, Lowe JB. Oocyte Galα1,3Gal epitopes implicated in sperm adhesion to the zona pellucida glycoprotein ZP3 are not required for fertilization in the mouse. J. Biol. Chem. 1995; 270:21437–21440. [PubMed: 7545161]
28. Tanemura M, Yin D, Chong AS, Galili U. Differential immune responses to α-gal epitopes on xenografts and allografts: implications for accommodation in xenotransplantation. J. Clin. Invest. 2000; 105:301–310. [PubMed: 10675356]
29. Abdel-Motal U, Wang S, Lu S, Wigglesworth K, Galili U. Increased immunogenicity of human immunodeficiency virus gp120 engineered to express Galα1-3Galβ1-4GlcNAc-R epitopes. J. Virol. 2006; 80:6943–6951. [PubMed: 16809300]
30. Abdel-Motal UM, Wigglesworth K, Galili U. Mechanism for increased immunogenicity of vaccines that form in vivo immune complexes with the natural anti-Gal antibody. Vaccine. 2009; 27:3072–3082. [PubMed: 19428921]
31. LaTemple DC, Abrams JT, Zhang SY, Galili U. Increased immunogenicity of tumor vaccines complexed with anti-Gal: studies in knockout mice for α1,3galactosyltransferase. Cancer Res. 1999; 59:3417–3423. [PubMed: 10416604]
32. Manches O, Plumas J, Lui G, Chaperot L, Molens JP, Sotto JJ, Bensa JC, Galili U. Anti-Gal-mediated targeting of human B lymphoma cells to antigen-presenting cells: a potential method for immuno-therapy using autologous tumor cells. Haematologica. 2005; 90:625–634. [PubMed: 15921377]
33. Galili U, Wigglesworth K, Abdel-Motal UM. Intratumoral injection of α-gal glycolipids induces xenograft-like destruction and conversion of lesions into endogenous vaccines. J. Immunol. 2007; 178:4676–4687. [PubMed: 17372027]
34. Eto T, Ichikawa Y, Nishimura K, Ando S, Yamakawa T. Chemistry of lipid of the posthemyolytic residue or stroma of erythrocytes. XVI. Occurrence of ceramide pentasaccharide in the membrane of erythrocytes and reticulocytes of rabbit. J. Biochem. 1968; 64:205–213. [PubMed: 4304380]
35. Stellner K, Saito H, Hakomori S. Determination of aminosugar linkage in glycolipids by methylation. Aminosugar linkage of ceramide pentasaccharides of rabbit erythrocytes and of Forssman antigen. Arch. Biochem. Biophys. 1973; 155:464–472.
36. Dabrowski U, Hanfland P, Egge H, Kuhn S, Dabrowski J. Immunochemistry of I/i-active oligo- and polyglycosylceramides from rabbit erythrocyte membranes. Determination of branching patterns of a ceramide pentadecasaccharide by 1H nuclear magnetic resonance. J. Biol. Chem. 1984; 259:7648–7651. [PubMed: 6736021]
37. Egge H, Kordowicz M, Peter-Katalinić J, Hanfland P. Immuno-chemistry of I/i-active oligo- and polyglycosylceramides from rabbit erythrocyte membranes. Characterization of linear, di-, and triantennary neolactoglycosphingolipids. J. Biol. Chem. 1985; 260:4927–4935. [PubMed: 3857231]
38. Hanfland P, Kordowicz M, Peter-Katalinić J, Egge H, Dabrowski J, Dabrowski U. Structure elucidation of blood group B-like and I-active ceramide eicosa- and pentacosasaccharides from

rabbit erythrocyte membranes by combined gas chromatography-mass spectrometry; electron-impact and fast-atom-bombardment mass spectrometry; and two-dimensional correlated, relayed-coherence transfer, and nuclear Overhauser effect 500-MHz 1H-n.m.r. spectroscopy. Carbohydr. Res. 1988; 178:1–21. [PubMed: 3191503]

39. Honma K, Manabe H, Tomita M, Hamada A. Isolation and partial structural characterization of macroglycolipid from rabbit erythrocyte membranes. J. Biochem. 1981; 90:1187–1196. [PubMed: 7309715]
40. Galili U, Wigglesworth K, Abdel-Motal UM. Accelerated healing of skin burns by anti-Gal/α-gal liposomes interaction. Burns. 2010; 36:239–251. [PubMed: 19501971]
41. Byrne GW, Stalboerger PG, Davila E, Heppelmann CJ, Gazi MH, McGregor HC, LaBreche PT, Davies WR, Rao VP, Oi K, et al. Proteomic identification of non-Gal antibody targets after pig-to-primate cardiac xenotransplantation. Xenotransplantation. 2008; 15:268–276. [PubMed: 18957049]
42. Galili U. The α-gal epitope and the anti-Gal antibody in xenotransplantation and in cancer immunotherapy. Immunol. Cell Biol. 2005; 83:674–686. [PubMed: 16266320]
43. Hamadeh RM, Galili U, Zhou P, Griffis JM. Anti-α-galactosyl immunoglobulin A (IgA), IgG, and IgM in human secretions. Clin. Diagn. Lab. Immunol. 1995; 2:125–131. [PubMed: 7697518]
44. Parker W, Bruno D, Holzknecht ZE, Platt JL. Characterization and affinity isolation of xenoreactive human natural antibodies. J. Immunol. 1994; 153:3791–3803. [PubMed: 7930596]
45. Vorauer-Uhl K, Fürnschlief E, Wagner A, Ferko B, Katinger H. Reepithelialization of experimental scalds effected by topically applied su-peroxide dismutase: controlled animal studies. Wound Repair Regen. 2002; 10:366–371. [PubMed: 12453140]
46. Plock JA, Rafatmehr N, Sinovcic D, Schnider J, Sakai H, Tsuchida E, Banic A, Erni D. Hemoglobin vesicles improve wound healing and tissue survival in critically ischemic skin in mice. Am. J. Physiol. Heart Circ. Physiol. 2009; 297:H905–H910. [PubMed: 19574491]
47. Jeschke MG, Herndon DN. The combination of IGF-I and KGF cDNA improves dermal and epidermal regeneration by increased VEGF expression and neovascularization. Gene Ther. 2007; 14:1235–1242. [PubMed: 17538636]
48. Roy S, Khanna S, Rink C, Biswas S, Sen CK. Characterization of the acute temporal changes in excisional murine cutaneous wound inflammation by screening of the wound-edge transcriptome. Physiol. Genomics. 2008; 34:162–184. [PubMed: 18460641]
49. Kelley JL, Suenram CA, Rozek MM, Schwartz CJ. Influence of hypercholesterolemia and cholesterol accumulation on rabbit carrageenan granuloma macrophage activation. Am. J. Pathol. 1988; 131:539–546. [PubMed: 2837904]
50. Aguiar-Passeti T, Postol E, Sorg C, Mariano M. Epithelioid cells from foreign-body granuloma selectively express the calcium-binding protein MRP-14, a novel down-regulatory molecule of macrophage activation. J. Leukoc. Biol. 1997; 62:852–858. [PubMed: 9400827]
51. Galili U. Immune response, accommodation, and tolerance to transplantation carbohydrate antigens. Transplantation. 2004; 78:1093–1098. [PubMed: 15502700]
52. Sen CK, Gordillo GM, Roy S, Kirsner R, Lambert L, Hunt TK, Gottrup F, Gurtner GC, Longaker MT. Human skin wounds: a major and snowballing threat to public health and the economy. Wound Repair Regen. 2009; 17:763–771. [PubMed: 19903300]
53. Orenstein A, Kachel E, Zuloff-Shani A, Paz Y, Sarig O, Haik J, Smolinsky AK, Mohr R, Shinar E, Danon D. Treatment of deep sternal wound infections post-open heart surgery by application of activated macrophage suspension. Wound Repair Regen. 2005; 13:237–242. [PubMed: 15953041]
54. Galili U, Tibell A, Samuelsson B, Rydberg L, Groth CG. Increased anti-Gal activity in diabetic patients transplanted with fetal porcine islet cell clusters. Transplantation. 1995; 59:1549–1556. [PubMed: 7539957]
55. Baumann BC, Stussi G, Huggel K, Rieben R, Seebach JD. Reactivity of human natural antibodies to endothelial cells from Galα(1,3)Galdeficient pigs. Transplantation. 2007; 83:193–201. [PubMed: 17264816]
56. Galili U, Ishida H, Tanabe K, Toma H. Anti-Gal A/B, a novel anti-blood group antibody identified in recipients of ABO-incompatible kidney allografts. Transplantation. 2002; 74:1574–1580. [PubMed: 12490791]

57. Crainic K, Durigon M, Oriol R. ABO tissue antigens of Egyptian mummies. Forensic Sci. Int. 1989; 43:113–124. [PubMed: 2691370]

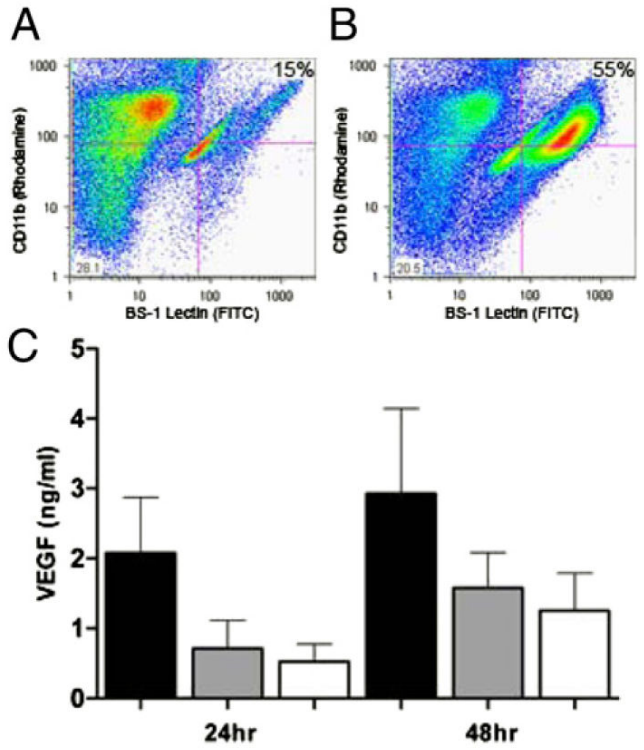

FIGURE 1.

Binding of anti-Gal Ab-coated α-gal liposomes to macrophages induces macrophage activation. αGT KO mouse peritoneal macrophages were incubated for 1 h at 4°C with α-gal liposomes (1.0 mg/ml) (*A*) or with anti-Gal Ab-coated α-gal liposomes (*B*). Binding of liposomes to macrophages was determined by flow cytometry with FITC-BS lectin (green: binding to α-gal liposomes) and with rhodamine–anti-CD11b (red: specific for macrophages). The proportion of double-stained cells representing α-gal liposomes bound to macrophages is indicated in the upper right corner. Data are representative of three independent studies. Number of stained cells increased in yellow and green areas and was the highest in red areas. *C*, Secretion of VEGF by peritoneal macrophages cocultured with anti-Gal Ab-coated α-gal liposomes (black columns), non-Ab–coated α-gal liposomes (gray columns), or no liposomes (white columns). VEGF was quantified in culture media after 24 or 48 h (mean + SD from four mice/group). VEGF secretion by macrophages incubated with anti-Gal Ab-coated α-gal liposomes was significantly greater than in the other two groups at 24 h. $p < 0.05$.

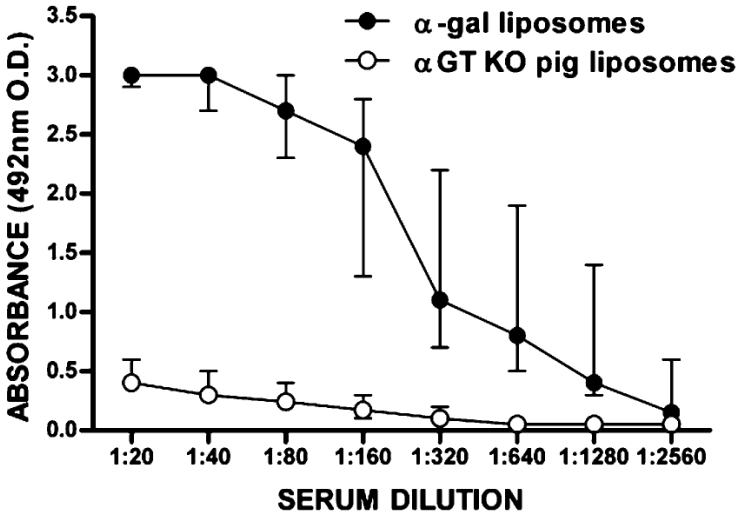

FIGURE 2.

Binding of anti-Gal IgG in αGT KO mouse serum to α-gal liposomes or to αGT KO pig liposomes coating ELISA wells. Data are presented as OD as a function of serum dilution (circles represent median, and lines represent the range of values).

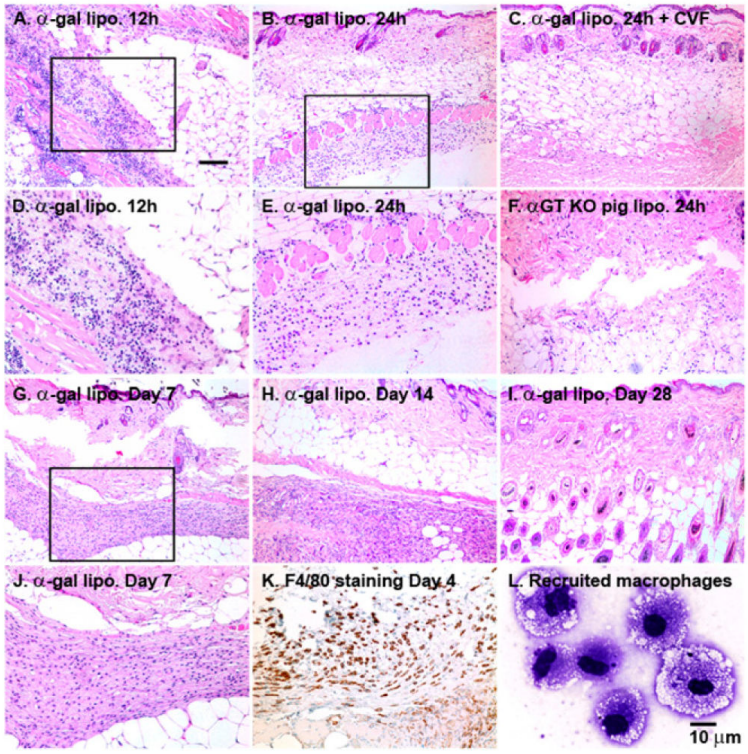

FIGURE 3.

Recruitment of cells following s.c. injection of 10 mg α-gal liposomes in αGT KO mouse skin. *A*, Twelve hours postinjection. Empty areas likely represent injected liposomes that were dissolved during the staining process. *B*, Twenty-four hours postinjection. *C*, Twenty-four hours postinjection of α-gal liposomes and 20 μg CVF. *D*, Enlargement of area outlined in *A*, showing recruited neutrophils. *E*, Enlargement of area outlined in *B*, indicating that most (>85%) of the cells have the morphology of macrophages. *F*, Twenty-four hours postinjection of 10 mg αGT KO pig liposomes (i.e., liposomes that lack α-gal glycolipids). Seven (*G*), 14 (*H*), and 28 (*I*) d postinjection of α-gal liposomes. *J*, Enlargement of area outlined in *G*, indicating that the mass of cells by the injection site is comprised of large macrophages containing multiple vacuoles that represent internalized phagocytosed α-gal liposomes. *K*, Ninety-six hours postinjection. The section was immunostained with HRP–anti-4/F80 Ab, which stains macrophages brown, and counterstained with hematoxylin. *L*, Morphology of individual recruited macrophages 7 d postinjection. The multiple vacuoles represent the anti-Gal Ab-coated α-gal liposomes internalized by the macrophages. For the purpose of orientation, the epidermis is shown in the upper areas of *B*, *C*, and *G–I*. Each figure is representative of five mice/group. *A–C* and *F–I*, H&E, original magnification ×100; *D*, *E*, *J*, and *K*, H&E, original magnification×200; *L*, H&E, original magnification ×1000. *A*, Scale bar, 100 μm; *L*, scale bar, 10 μm.

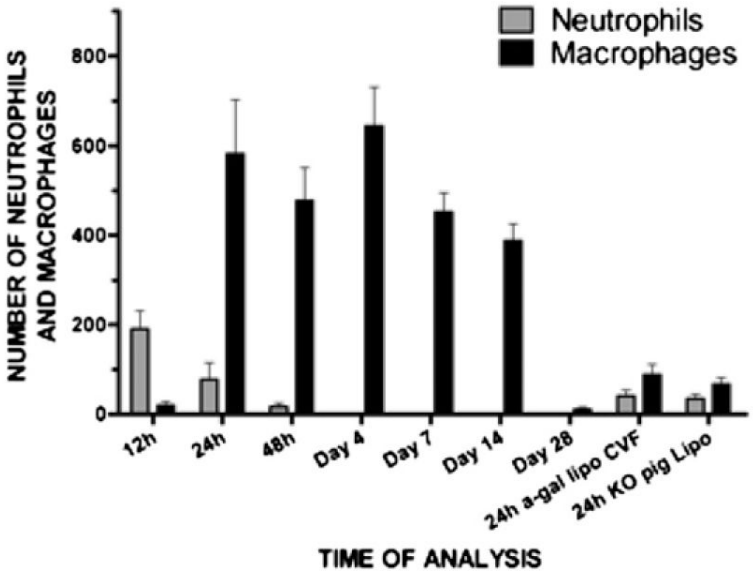

FIGURE 4.

Recruitment of neutrophils and macrophages by 10 mg of liposomes injected s.c. in 0.1 ml suspension into αGT KO mice. In some experiments, α-gal liposomes were coinjected with 20 μg CVF (which inhibits complement activity). Liposomes produced from α1,3GT KO pig RBCs (liposomes that lack α-gal epitopes) are referred to as KO pig Lipo. Number of infiltrating cells was determined in histological sections by counting cells within a rectangular area marked in a microscope lens at a magnification of ×400, corresponding to a 100 × 200-μm area. The differences in the number of macrophages between day 1 and day 14 are not statistically significant. Mean + SD from five mice/group.

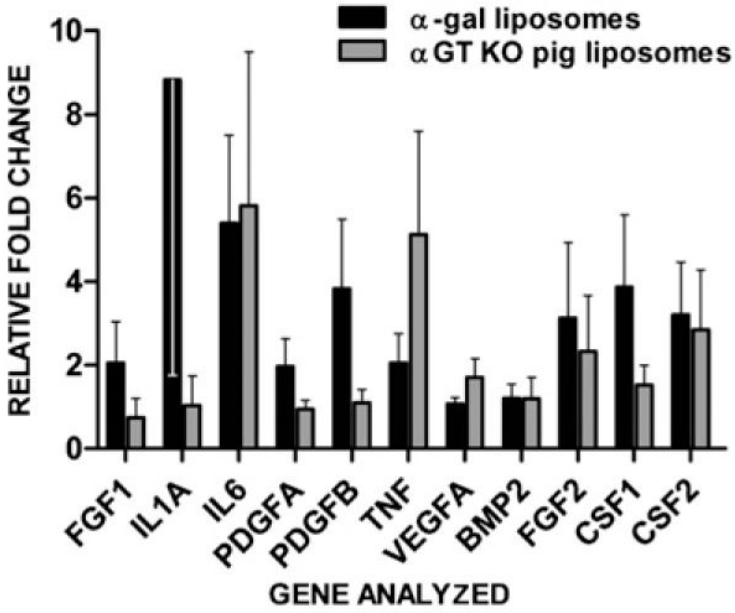

FIGURE 5.

Cytokine gene expression in αGT KO mouse skin injected with liposomes, as measured by q-RT-PCR. Fold changes in expression of the various cytokine genes in RNA extracts of αGT KO mice injected in the skin with α-gal liposomes and harvested after 48 h compared with saline-injected skin as control (n = 5, black columns). Skin specimens from αGT KO mice injected with 10 mg αGT KO pig liposomes served as a specificity control (n = 4, gray columns). Data are mean + SD, with the exception of *Il1a* in α-gal liposome-treated wounds, for which it is mean − SD.

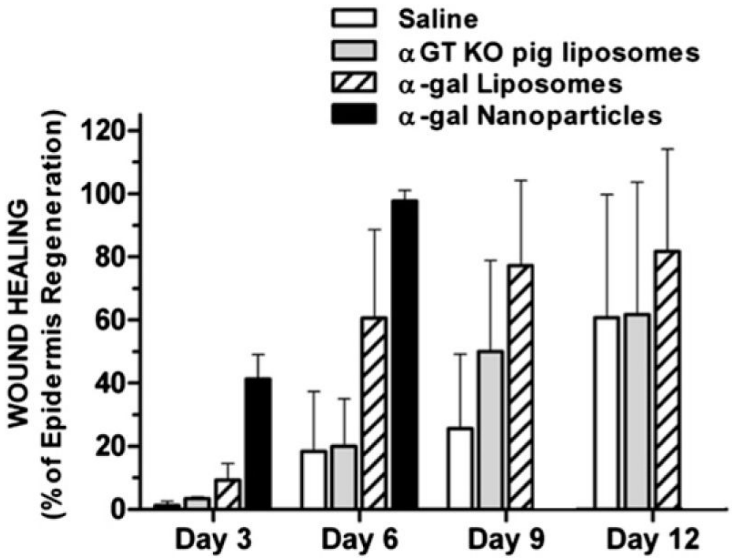

FIGURE 6.

Wound healing at different time points after excisional wound formation and topical application of dressing covered with 10 mg of α-gal liposomes (striped columns), 10 mg of αGT KO pig liposomes lacking α-gal epitopes (gray columns), or saline (open columns). Healing of wounds treated with α-gal nanoparticles is shown in black columns. Extent of wound healing is presented as the percentage of the wound area covered with regenerating epidermis. On day 3, $n = 11$ for all groups. On day 6, $n = 20$ for mice with wounds treated with α-gal liposomes or with saline and $n = 11$ for mice treated with α-gal nanoparticles and those treated with αGT KO pig liposomes. On day 9, $n = 8$ for all groups, whereas $n = 11$ for all groups on day 12. Data are presented as mean + SD. A statistically significant difference was observed in mice treated with α-gal nanoparticles compared with the other groups on days 3 and 6. $p < 0.05$.

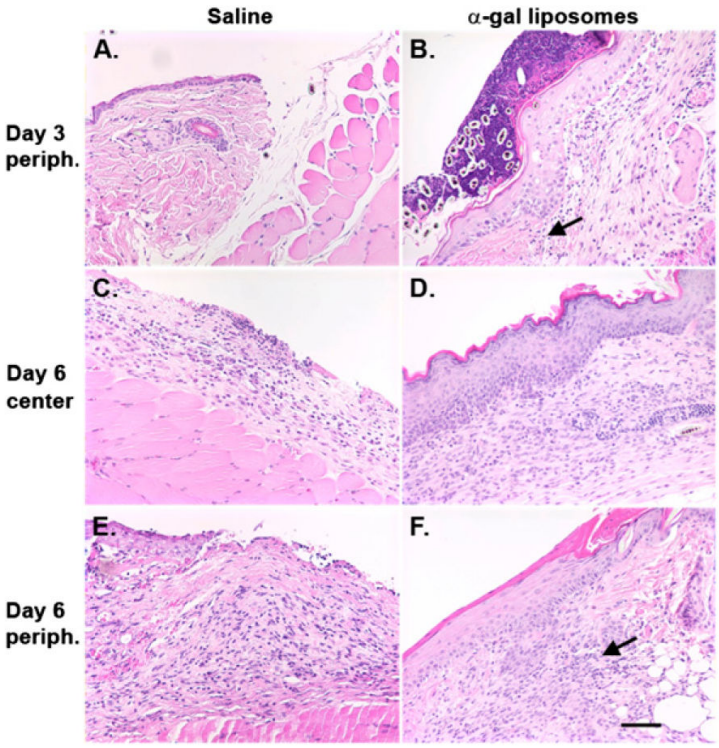

FIGURE 7.

Healing of representative excisional wounds treated with spot bandage dressing covered with 10 mg of α-gal liposomes or with saline. *A*, Control wound treated with saline dressing for 3 d. Panniculus carnosus muscle layer is exposed where epidermis and dermis were removed. No significant cell infiltration is observed. *B*, Wound treated for 3 d with α-gal liposomes. Note the multilayered proliferating epidermis at the periphery of the wound and infiltration of macrophages in the regenerating dermis. The platelet plug is present above the healing wound. Arrow marks the wound edge. *C*, Day-6 saline-treated wound (center of the wound). Regenerating thin dermis over panniculus carnosus is filled with macrophages. No regenerating epidermis is observed. *D*, Day-6 wound treated with α-gal liposomes (center of the wound). Note that multilayered regenerating epidermis covers the entire area of the wound, and many macrophages infiltrate the dermis. *E*, Day-6 saline-treated wound (periphery of the wound). The regenerating epidermis in the lower left area does not cover the entire wound. The dermis is filled with macrophages. *F*, Day-6 wound treated with α-gal liposomes (periphery of the wound). The uninjured skin is observed in the right area. The dermis of the wound is filled with macrophages. Arrow marks the wound bed. Pink stratum corneum is observed over the regenerating epidermis. Scale bar, 50 μm. *A*, H&E, original magnification ×100; *B*–*F*, H&E, original magnification ×200. Specimens are representative of 7 mice treated with α-gal liposome (complete wound closure) and of 20 mice treated with saline.

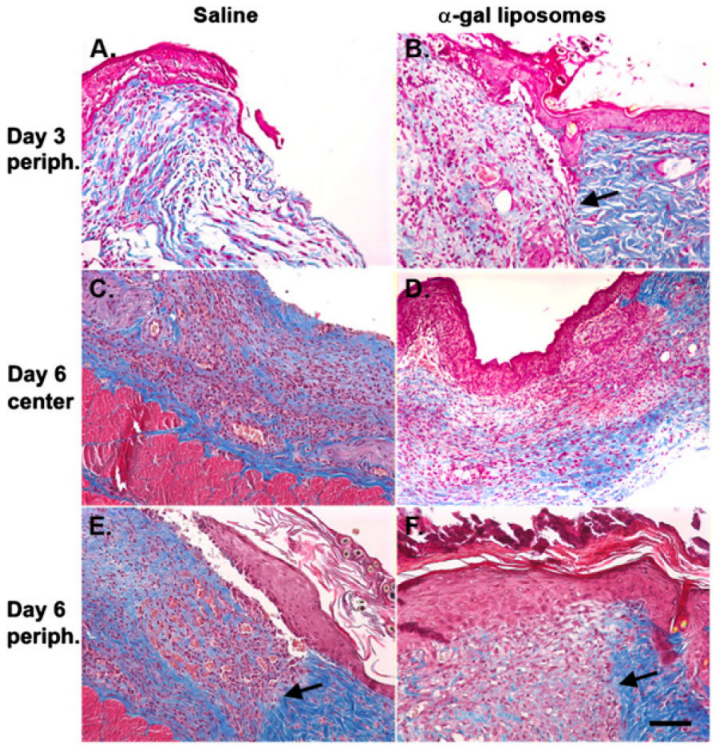

FIGURE 8.

Trichrome staining of regenerating dermis in the skin wounds treated with dressing (spot bandages) covered with saline (*A*, *C*, *E*) or with 10 mg of α-gal liposomes (*B*, *D*, *F*), as detailed in Fig. 7. Collagen is stained blue, and the various cells are stained purple. The border of the wound bed between uninjured and regenerating tissues is marked with arrows in *B*, *E*, and *F*. *A*, *C*, and *D*, Original magnification ×100; *B*, *E*, and *F*, original magnification ×200. Scale bar, 50 μm. Specimens are representative of 7 mice treated with α-gal liposome (complete wound closure) and of 20 mice treated with saline.

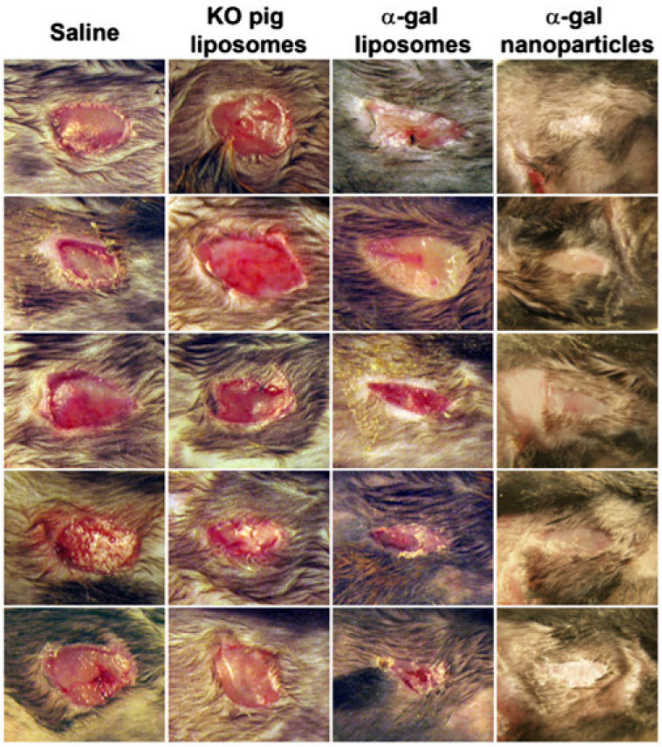

FIGURE 9.

Gross appearance of day-6 excisional wounds treated with dressing (spot bandages) covered with saline, αGT KO pig liposomes, α-gal liposomes, and α-gal nanoparticles (2–4-fold magnification). Note that wounds treated with saline or αGT KO pig liposomes displayed minimal healing. In contrast, wounds treated with α-gal liposomes displayed 30–80% healing, and those treated with α-gal nanoparticles displayed 95–100% healing. Wounds are from representative mice presented in Fig. 6. The wound observed in the lower left of the first mouse in the group treated with α-gal nanoparticles is due to rubbing of the adhesive tape on the skin and is not related to the actual wound performed by excision and that displayed 100% healing.

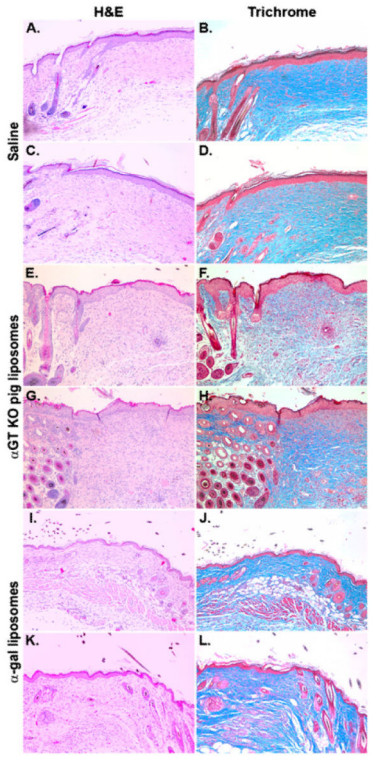

FIGURE 10.

α-Gal liposome treatment decreases scar formation. Wounds treated for 28 days with saline (*A–D*) or αGT KO pig liposome (*E–H*) developed a scar characterized by dense connective tissue containing multiple fibroblasts, thick epidermis, and no skin appendages, such as hair and sebaceous glands (*right area* in *A–H*). In contrast, wounds treated for 28 d with α-gal liposomes (*I–L*) displayed restoration of normal skin histology, including thin epidermis, loose connective tissue in the dermis, and the appearance of hair and sebaceous glands, as well as fat cells in the hypodermis. H&E and trichrome (collagen is stained blue), original magnification ×100. Specimens in each group are two representative mice of five mice/group.